J. Fluid Mech. (2006), *vol.* 552, *pp.* 83–97.
doi:10.1017/S0022112005008529 Printed in the United Kingdom

Inertial effects on Saffman–Taylor viscous fingering

By CHRISTOPHE CHEVALIER[1,3], MARTINE BEN AMAR[2], DANIEL BONN[2,4] AND ANKE LINDNER[1]

[1]Laboratoire de Physique et Mécanique des Milieux Hétérogènes, UMR 7636 CNRS, Université Paris 6, Ecole Supérieure de Physique et de Chimie Industrielles, 10 rue Vauquelin, 75231 Paris cedex 05, France

[2]Laboratoire de Physique Statistique, UMR 8550 CNRS, Ecole Normale Supérieure, 24 rue Lhomond, 75231 Paris cedex 05, France

[3]Ecole Nationale des Ponts et Chaussées, 6-8 avenue Blaise Pascal, Cité Descartes, Champs sur Marne, 77455 Marne-la-Vallée cedex 2, France

[4]Van der Waals-Zeeman Institute, University of Amsterdam, Valckenierstraat 65, 1018 XE Amsterdam, the Netherlands

(Received 2 June 2005 and in revised form 21 September 2005)

For the Saffman–Taylor instability, the inertia of the fluid may become important for high finger speeds. We investigate the effects of inertia on the width of the viscous fingers experimentally. We find that, due to inertia, the finger width can increase with increasing speed, contrary to what happens at small Reynolds number Re. We find that inertial effects need to be considered above a critical Weber number We. In this case it can be shown that the finger width is governed by a balance between viscous forces and inertia. This allows us to define a modified control parameter $1/B'$, which takes the corrections due to inertia into account; on rescaling the experimental data with $1/B'$, they all collapse onto the universal curve for the classical Saffman–Taylor instability. Subsequently, we try to rationalize our observations. Numerical simulations, taking into account a modification of Darcy's law to include inertia, are found to only qualitatively reproduce the experimental findings, pointing to the importance of three-dimensional effects.

1. Introduction

Viscous fingering has received much attention as an archetype of pattern-formation problems and as a limiting factor in the recovery of crude oil (see Saffman & Taylor 1958; Bensimon *et al.* 1986; Homsy 1987; Couder 1991). Viscous fingers form in a thin linear channel or Hele-Shaw cell when a fluid pushes a more viscous fluid. The interface between the fluids develops an instability leading to the formation of finger-like patterns. The viscous fingering instability has been studied extensively over the past few decades, both theoretically and experimentally.

For the classical Saffman–Taylor instability the width of the finger is governed by the competition between viscous and capillary forces: viscous forces tend to narrow the finger whereas capillary forces tend to widen it. When air pushes a viscous fluid, as is usually the case, the relative finger width is thus determined by the capillary number $Ca = \eta U/\gamma$ (with η the fluid viscosity, U the velocity and γ the surface tension), the ratio between viscous and capillary forces. In the vast majority of cases that have been studied so far, inertial forces are negligible. The importance of inertia is determined by the relative importance of the inertial and viscous forces, quantified

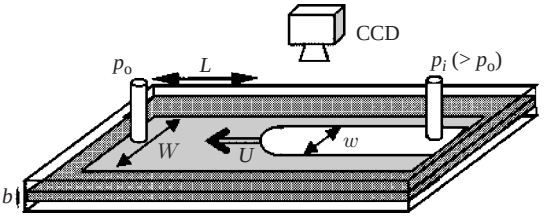

FIGURE 1. Schematic drawing of the experimental set-up.

by the Reynolds number $Re = \rho U b/\eta$, with ρ the fluid density, and b the plate spacing of the Hele-Shaw cell in which the experiments are conducted. In most studies of the instability, b is small, and the fluids considered both in applications as well as in experimental studies are typically high-viscosity oils. This automatically leads to small Reynolds numbers ($Re \ll 1$), so that inertial effects may be neglected.

More recently viscous fingering has been studied in non-Newtonian fluids using for example polymer solutions (see Smith *et al.* 1992; Bonn *et al.* 1995; Lindner, Bonn & Meunier 2000; Vlad & Maher 2000; Kawaguchi, Hibino & Kato 2001; Lindner *et al.* 2002). For the dilute polymer solutions used in a number of these studies, the shear viscosity of the water-based solutions is typically close to the water viscosity, and consequently the Reynolds number may – and does – become larger than unity. This means that inertia may become important, and needs to be disentangled from the observed non-Newtonian flow effects. Also recently, corrections to Darcy's law have been developed incorporating inertial effects (see Gondret & Rabaud 1997; Ruyer-Quil 2001). Darcy's law relates the pressure gradient to the fluid velocity and is one of the fundamental equations of the Saffman–Taylor instability; if inertial corrections could simply be included in a modified Darcy's law, this would greatly facilitate the understanding of the effect of inertia on the instability. These recent developments suggest that a better understanding of the Newtonian fingering instability for high Reynolds numbers is both necessary and feasible.

In this paper we explore the Saffman–Taylor instability for Newtonian fluids for Reynolds numbers up to $Re = 100$. To do so, we use low-viscosity silicone oils, pushed by air. The paper is organized as follows. In § 2 we will recall the basic equations for the Saffman–Taylor instability and introduce the corrections due to inertia. Section 3 describes the set-up and experimental methods. In § 4 the experimental results concerning the finger widths as well as the validity of Darcy's law are presented and discussed. In § 5 we will introduce some theoretical elements as well as numerical simulation and compare them to the experimental results. Section 6 gives a summary of the obtained results.

2. Theory and equations

2.1. *Presentation and review of classical Saffman–Taylor instability*

We study the Saffman–Taylor instability in a thin linear channel or Hele-Shaw cell (see figure 1). The width of the cell W is chosen to be large compared to the channel thickness b and we thus work with high aspect ratios W/b. The cell is filled with a viscous fluid which is subsequently pushed by air. The viscosity and the density of air will be neglected throughout the paper.

When air pushes the viscous fluid due to an imposed pressure gradient ∇P, initially flat interface between the two fluids destabilizes. This destabilization leads to the

formation of a so-called viscous finger; in steady state a stationary finger of width w propagating at a velocity U is found to occupy a fraction of the cell width: the relative finger width is defined as $\lambda = w/W$.

For Newtonian fluids, the motion of a fluid in the Hele-Shaw cell is described by the two-dimensional velocity field $\boldsymbol{u}$ averaged through the thickness of the cell. It is given by Darcy's law, which relates the local pressure gradient to the velocity within the fluid as

$$\boldsymbol{u} = -\frac{b^2}{12\eta}\nabla p. \tag{2.1}$$

It follows immediately that, if the fluid is incompressible, the pressure field satisfies Laplace's equation:

$$\Delta p = 0. \tag{2.2}$$

The pressure field is calculated within the driven fluid, together with a pressure jump over the interface due to the surface tension:

$$\delta p = \gamma/R, \tag{2.3}$$

with R the radius of curvature of the interface, again employing a two-dimensional approximation, as was justified in the limit of small capillary numbers by Park & Homsy (1984), and Reinelt & Saffman (1985).

The other boundary conditions are the continuity condition, which implies that the normal velocity at both sides of the interface is equal:

$$\boldsymbol{U}\cdot\boldsymbol{n} = \boldsymbol{u}\cdot\boldsymbol{n}, \tag{2.4}$$

with $\boldsymbol{n}$ being the normal vector to the interface, and a far-field value for the pressure. Supplemented with these boundary conditions, (2.1), (2.2) and (2.3) constitute the complete set of equations to be solved in order to obtain the complete finger shape for a given pressure gradient; and thus also its width.

For characterizing the instability quantitatively most studies have focused on the width of the finger w relative to the channel width W, $\lambda = w/W$, as a function of the finger velocity. It follows from the above that the finger width is determined by the capillary number; one thus anticipates that the relative width of the viscous fingers decreases with increasing finger velocity. This is indeed what is observed experimentally; in addition, for very large values of Ca, λ does not go to zero but reaches a limiting value of about half the channel width. It also follows from the boundary conditions and (2.1) to (2.3) that the control parameter for the fingering problem is $1/B = 12(W/b)^2 Ca$ with W/b the aspect ratio of the Hele-Shaw cell. When scaled on $1/B$, measurements of λ for different systems all fall on the same universal curve. In the ideal, Newtonian, two-dimensional situation $1/B$ is consequently the only parameter that determines the finger width (see Saffman & Taylor 1958; McLean & Saffman 1981; Combescot *et al.* 1986; Hong & Langer 1986; Shraiman 1986).

2.2. *Corrections of Darcy's law due to inertia*

When inertial forces have to be taken into account, both the Reynolds number $Re = \rho U b/\eta$ and the Weber number $We = \rho U^2 b/\gamma$ (the ratio of inertial forces to capillarity forces) become important. We will now, as a first step, discuss how corrections due to inertia can be included in Darcy's law.

Modifications of Darcy's law were first proposed by Gondret & Rabaud (1997) for parallel flow in a Hele-Shaw cell: they establish corrections by averaging inertia in the third dimension, i.e. they average over the direction of the plate spacing b,

allowing them to derive a new nonlinear two-dimensional equation for the velocity field. Ruyer-Quil (2001) suggests an improved correction starting from the three-dimensional Navier–Stokes equation. Inertial corrections are introduced in a perturbative fashion; using in addition a polynomial approximation to the velocity field, Ruyer-Quil proposes a modified two-dimensional Darcy's law of the form:

$$\rho\left(\alpha\frac{\partial \boldsymbol{u}}{\partial t}+\beta\boldsymbol{u}\cdot\nabla\boldsymbol{u}\right)=-\nabla p-\frac{12\eta}{b^2}\boldsymbol{u}, \tag{2.5}$$

with $\alpha=6/5$ and $\beta=54/35$ and $\boldsymbol{u}$ the depth-averaged velocity. Plouraboue & Hinch (2002) also calculated inertial corrections to Darcy's law and arrived at a similar type of equation, but with slightly different coefficients. This equation leads to a better agreement between the linear stability analysis and the experimental data of Gondret & Rabaud for the Kelvin–Helmholtz instability up to not too large Reynolds numbers. The values of α and β may vary depending on the way the averaging in the third dimension is done, but are always of order of 1.

Scaling length on W, time on W/U and pressure on $12\eta UW/b^2$ gives the following dimensionless equation:

$$Re^*\left(\alpha\frac{\partial \boldsymbol{u}^*}{\partial t^*}+\beta\boldsymbol{u}^*\cdot\nabla^*\boldsymbol{u}^*\right)=-\nabla^* p^*-\boldsymbol{u}^*,\quad \text{where}\quad Re^*=\frac{1}{12}\frac{b}{W}\frac{\rho Ub}{\eta}=\frac{b}{12W}Re. \tag{2.6}$$

Re^* is a modified Reynolds number, in the same way as the classical control parameter of the Saffman–Taylor instability $1/B$ is a modified capillary number.

We can also introduce another number describing the relative importance of inertia and capillarity in the geometry of the Hele-Shaw, a modified Weber number:

$$We^*=\frac{\rho U^2W}{\gamma}=\frac{W}{b}We. \tag{2.7}$$

One important remark is that if one considers stationary and spatially uniform two-dimensional flow in our Hele-Shaw cell, it follows from (2.5) that there are no corrections due to inertia, since $\partial\boldsymbol{u}/\partial t$ and $\boldsymbol{u}\cdot\nabla\boldsymbol{u}$ are both zero. This will be the case in our fingering experiments far away from the moving interface and leads to the classical Darcy law; we thus anticipate that it might remain valid even for relatively high Re.

3. Experimental

We use a linear Hele-Shaw cell consisting of two glass plates separated by a thin Mylar spacer. The plates are horizontal and clamped together in order to obtain a regular thickness b of the channel. The thickness of the glass plates is chosen to be 2 cm in order to avoid any bending. The aspect ratio of the channel can be varied; we worked with different plate spacings b and widths W, the length of the channel always being 1 m. The cell is filled with silicone oil and compressed air is used as the less-viscous driving fluid.

The silicone oils used were Rhodorsil 47V05, 47V10, 47V20 and 47V100 from Rhodia Silicones. Rheological measurements on a Reologica Stress-Tech rheometer confirmed the values of the viscosities η of 5, 10, 20 and 100 mPa s respectively, with no deviations larger than 4 %. We also used 47V02, with viscosity measured to be 2.8 mPa s. The surface tension γ and the density ρ of the silicone oils are $19.5\pm1\,\mathrm{mN\,m^{-1}}$ and $0.95\pm0.03\ 10^{-3}\,\mathrm{kg\,m^{-3}}$ as given by Rhodia Silicones.

	Thickness b	Width W	Aspect ratio W/b
Geometry 1	0.25 mm	40 mm	160
Geometry 2	0.75 mm	80 mm	107
Geometry 3	0.75 mm	40 mm	53
Geometry 4	1.43 mm	40 mm	28

TABLE 1. Different cell geometries used in our experiments.

The fingers were driven by applying a constant pressure drop $\Delta p = p_i - p_o$ between the inlet and the outlet of the cell. Depending on the order of magnitude of the applied pressure drop two methods were used. For Δp larger than 3000 Pa we used compressed air and a pressure transducer at the entrance of the cell to fix p_i at the inlet of the cell. In this case, the outlet was maintained at atmospheric pressure $p_o = p_{atm}$ by an oil reservoir coupled to the cell. For Δp smaller than 3000 Pa, we obtained the pressure drop by lowering the oil reservoir at the outlet of the cell by a given distance, determining in this way p_o. In this case the inlet was maintained at atmospheric pressure $p_i = p_{atm}$.

The fingers were captured by a CCD camera, coupled to a data acquisition card (National Instruments) and a computer. This allowed measurements of the relative width $\lambda = w/W$ as a function of the velocity U of the finger tip. For each configuration (cell geometry and fluid viscosity) several experimental runs (between 10 and 20) were performed increasing the applied pressure drop and thus the finger velocity until destabilization of the finger occurred; all the finger widths reported here correspond to stable fingers.

In order to access high Reynolds numbers we not only varied the velocity of the finger and the viscosity of the fluid but also the thickness of the channel. We have thus worked with different channel geometries that are summarized in table 1.

The aspect ratio W/b varies from 28 (geometry 4) to 160 (geometry 1). Even though an aspect ratio of 28 is rather small it is sufficient to consider the experiment as being quasi-two-dimensional. It was observed that the results obtained for the high-viscosity fluids (and thus a situation where inertial effects can be neglected) show very little difference in finger widths. The small difference is due to film effects (see Tabeling & Libchaber 1986), as will be discussed in more detail below.

Experiments were performed in all geometries for the silicon oils 47V05, 47V10 and 47V20. The Silicon oil 47V02 was tested in geometries 2 and 3, whereas the silicon oil 47V100 was used in geometries 3 and 4. Finally, note that typical values of capillary number Ca in the experiments are between 0.01 (for V02) and 0.5 (for V100).

4. Presentation of the results

4.1. *Darcy's law*

Assuming the flow far away from a finger to be uniform, we expect that the classical Darcy law linking the gap-averaged fluid velocity V to the imposed pressure gradient ∇P in our Hele-Shaw cell remains valid for all of our experiments:

$$V = -\frac{b}{12\eta}\nabla P. \tag{4.1}$$

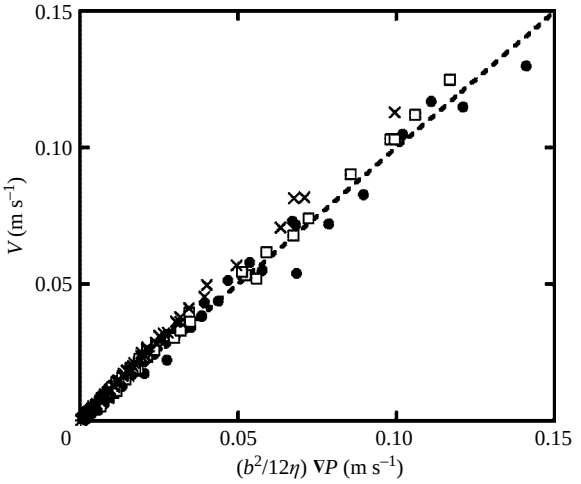

FIGURE 2. Velocity as a function of the applied pressure gradient for all viscosities (V02, V05, V10, V20 and V100) and different cell geometries: •, $b = 1.43$ mm $W = 4$ cm; ×, $b = 0.75$ mm $W = 4$ cm; □, $b = 0.75$ mm $W = 8$ cm; +, $b = 0.25$ mm $W = 4$ cm.

Mass conservation allows the velocity V of the fluid far away from the interface to be obtained from the measured finger velocity U simply by using $V = \lambda U$, if one neglects the thin wetting film left on the glass plates behind the finger. The imposed pressure gradient is calculated from $\nabla P = \Delta p/L$ where Δp is the measured applied pressure drop and L the distance between the finger tip and the exit of the cell.

In our experiments we reach high finger velocities and thus high capillary numbers Ca. The influence of the thin wetting film left on the plates may therefore become important and can no longer be neglected. It is taken into account using $V = \lambda U(1 - 2t/b)$, where t is the thickness of the wetting film, which we estimate using the empirical result of Tabeling & Libchaber (1986) and Tabeling, Zocchi & Libchaber (1987):

$$t = \kappa b[1 - \exp(-\gamma W/b)][1 - \exp(-\beta Ca^{2/3})], \tag{4.2}$$

with $\kappa \approx 0.119$, $\gamma \approx 0.038$ and $\beta \approx 8.58$. For our data, the correction $2t/b$ varies from 0.02 to 0.2. Note that this simple correction does not take into account an eventual modification of the film thickness by inertia. However it already improves the fit of the data significantly.

In this way, we can thus test the validity of Darcy's law. Figure 2 shows the velocity V represented as a function of $(b/12\eta)\nabla P$ for the different cell geometries and viscosities used. The dashed line represents the linear relation with slope unity expected from (4.1). We therefore conclude that the data are in excellent agreement with the classical Darcy law. This result holds even for high velocities where a significant effect of the inertial forces is observed on the width of the fingers, as will be discussed below. We have thus shown that for the range of Re tested in this paper there is, as was anticipated above, no effect of inertia on Darcy's law when considering the uniform flow far away from the finger. Note that this does not automatically imply that there are no corrections to the local relation between ∇p and the velocity near the finger tip.

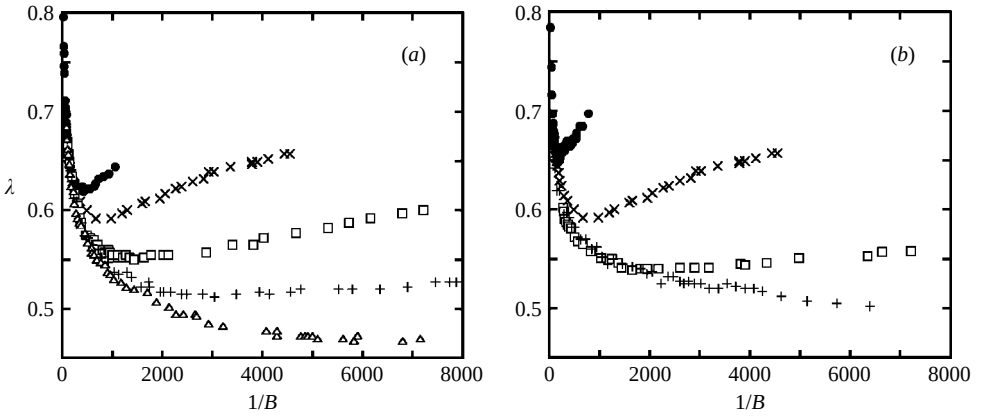

FIGURE 3. Results for the finger width λ as a function of the classical control parameter $1/B$: (*a*) for the geometry with $b = 0.75$ mm and $W = 4$ cm and different fluids: •, V02; ×, V05; □, V10; + V20; △, V100. (*b*) for the V05 fluid and different cell geometries: •, $b = 1.43$ mm $W = 4$ cm; ×, $b = 0.75$ mm $W = 4$ cm; □, $b = 0.75$ mm $W = 8$ cm; +, $b = 0.25$ mm $W = 4$ cm.

4.2. *Finger width*

4.2.1. *Relative finger width as a function of the classical control parameter*

Figures 3(*a*) and 3(*b*) represent the relative finger width as a function of the classical control parameter $1/B$ when varying the viscosity of the fluid for a given geometry – $b = 0.75$ mm, $W = 4$ cm, figure 3(*a*) – and when changing the geometry of the cell for a given fluid, silicon oil 47V05, figure 3(*b*). These figures show for low $1/B$ the classical decrease of the finger width with increasing $1/B$. However at a given value of $1/B$ which is different for different configurations, an increase of the relative finger width is observed. This surprising observation systematically appears at high Reynolds numbers, and we conclude that it must be related to inertial effects. Indeed, for a given geometry, only the fluid of highest viscosity gives results that agree with the classical Saffman–Taylor instability. In addition, deviations from the classical results arise at smaller $1/B$ for lower fluid viscosity. Finally, the data for a fixed viscosity but varying geometry (figure 3*b*) show that the increase of the finger width occurs for lower $1/B$ for a channel with a larger plate spacing. All these observations agree with the suggestion that the increase in finger width with increasing velocity is due to inertial effects.

Comparing the data for a fixed gap thickness ($b = 0.75$ mm) and two different channel widths ($W = 4$ and $W = 8$ cm) in figure 3(*b*), we conclude that the crossover value of $1/B$ also depends on the channel width W: it is observed to be smaller for smaller channel widths. This is still consistent with an increase of the Reynolds numbers (Re and Re^*): at a given $1/B$ and fixed η and b, a decrease of the channel width W leads to an increase of Re. This follows from the observation that W^2U is fixed and consequently Re varies as $1/W$ (Re^* as $1/W^3$).

We conclude that due to inertia our experimental results deviate from the classical results: we observe a regime of increasing finger width. This increase occurs at lower $1/B$ for lower viscosity, larger gap thickness or smaller gap width. It is also important to note that strong inertial effects are already observed at velocities below $0.08\ \mathrm{m\,s^{-1}}$ for all of our experiments and that even if strong changes in the behaviour are observed for the finger width, no deviations from the classical Darcy law are observed in this regime (figure 2).

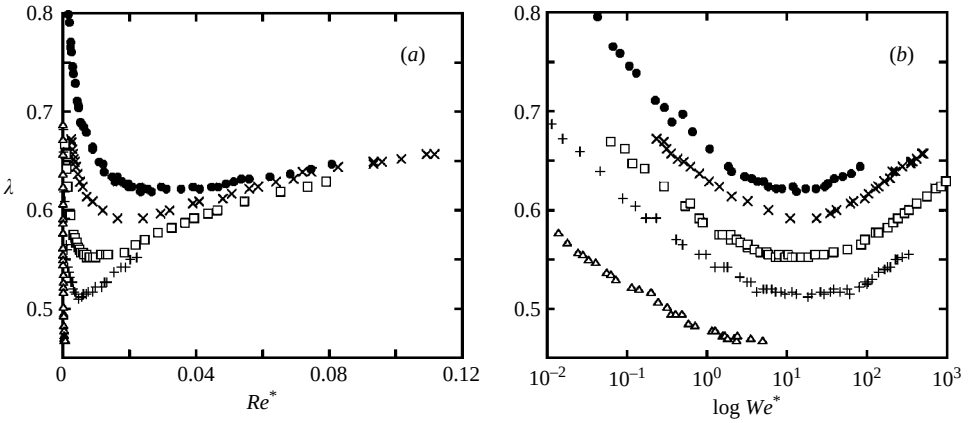

FIGURE 4. Results for the finger width λ as a function of (a) the modified Reynolds number $Re^*$and (b) the modified Weber number We^*, for the geometry with $b = 0.75$ mm and $W = 4$ cm and different fluids: •, V02; ×, V05; □, V10; + V20; △, V100.

We will now study the deviation from the classical result as a function of the modified Reynolds number Re^*. For concreteness, in the following we will focus on the data obtained when varying the viscosity for a given geometry ($b = 0.75$ mm, $W = 4$ cm). The results however are general and apply to the data from other experiments as well.

4.2.2. *Relative finger width as function of the modified Reynolds number Re^**

In figure 4(a), we plot the relative finger width as a function of the modified Reynolds number Re^*. The first observation is that the minimum of the curves (that signals the deviation from the classical results) is not fixed at the same value of Re^*. On the other hand for high Re^* all the curves tend towards a single master curve: the behaviour of the finger width seems to be governed by Re^* only. Data in other configurations (not shown here) confirm the existence of a universal λ–Re^*curve for high Re^*.

4.2.3. *Relative finger width as a function of the modified Weber number We^**

So far we can distinguish between two limiting cases. For low velocities, the results for the relative finger width fall on the universal curve of the classical Saffman–Taylor instability: they rescale with $1/B$. For high values of velocity, a second universal curve exists and the data rescale with Re^*. This suggests that the crossover between the two regimes may be given by the modified Weber number, combining Re^* and $1/B$:

$$We^* = Re^* 1/B = \frac{\rho U^2 W}{\gamma} = \frac{W}{b} We. \tag{4.3}$$

The experimental data support this conclusion. Figure 4(b) depicts the relative finger width as a function of the modified Weber number We^*. All experimental curves have a minimum located at the same value of We^*, at around $We^*_c \approx 15$, separating the two limiting behaviours.

Note that, although We^* governs the crossover, we observe no regime where the finger width is determined by a competition between capillary forces and inertia. In fact, when considering the dependence of the different forces on the velocity one finds that capillary forces scale as U^0, viscous forces as U^1 and inertial forces

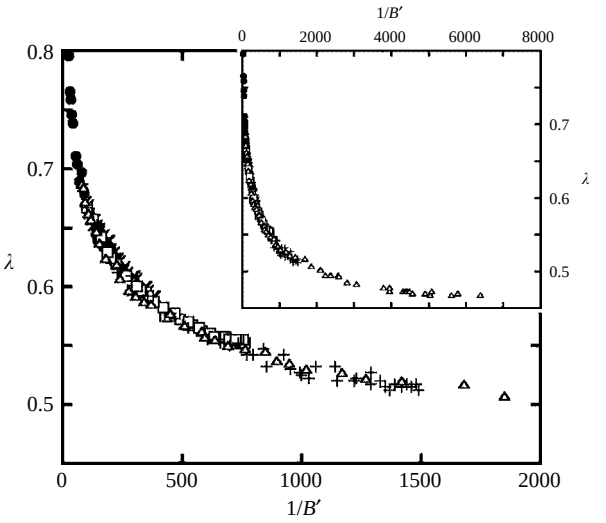

FIGURE 5. Results for the finger width λ (same data as figure 3*a*) as a function of the modified control parameter $1/B'$, for the geometry with $b = 0.75$ mm and $W = 4$ cm and different fluids: •, V02; ×, V05; □, V10; + V20; △, V100. (Inset: same data, but over a larger range of $1/B'$.)

as U^2. Consequently, the dominating forces at low velocity should be capillary and viscous forces (control parameter $1/B$) and at high velocity, viscous forces versus inertia (control parameter Re^*). This simple argument therefore explains that as a function of the velocity there is no regime where the finger width is given by We^*.

4.2.4. *Extension to a new global master curve*

It follows that the parameter We^* ($= Re^* 1/B$), that can be seen as the ratio between $1/B$ and $1/Re^*$, gives the relative importance of the two parameters with a crossover given by the critical value $We_c^* \approx 15$.

We can thus attempt to define a modified control parameter taking this crossover into account:

$$1/B' = 1/B\left(\frac{1}{1 + We^*/We_c^*}\right). \tag{4.4}$$

It is easy to see that this parameter tends to $1/B$ for low We^* ($We^* < We_c^*$) and towards We_c^*/Re^* for large We^* ($We^* > We_c^*$).

Figure 5 shows the experimental data already shown on figure 3(*a*), however now λ is plotted as a function of $1/B'$ for $We_c^* = 15$. The experimental data scale on a single universal curve when represented as a function of the modified control parameter. Moreover, and perhaps more surprisingly, this curve is identical to the classical result of McLean & Saffman (1981) on viscous fingering, experimentally represented by the data obtained for the most viscous oil where inertia plays no role. Note that when representing the data as a function of $1/B'$ they are folded back onto themselves.

Figures 6(*a*) and 6(*b*) summarize our results. On figure 6(*a*), all geometries and fluids are depicted, representing the relative finger width as a function of the classical control parameter $1/B$. Note that these data are obtained by varying not only the fluid viscosity but also the cell geometry by changing both the channel width and thickness. On figure 6(*b*), the same data are plotted as a function of $1/B'$, our modified control

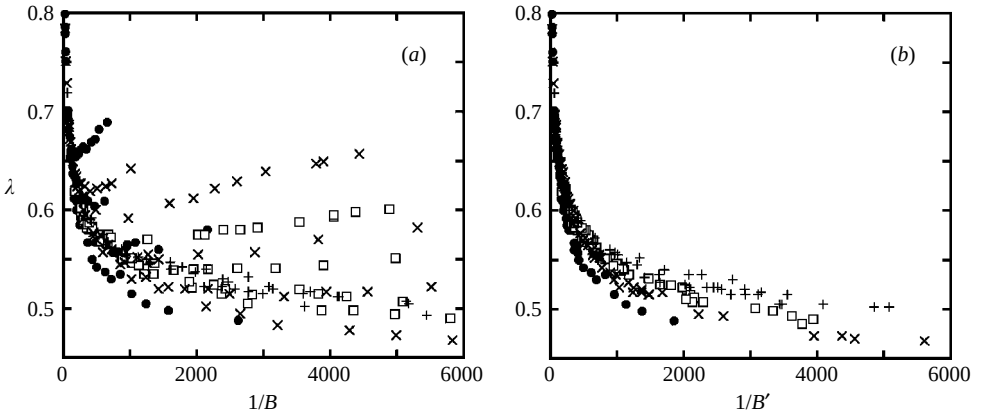

FIGURE 6. Results for the finger width λ as a function of (a) the classical control parameter $1/B$ and (b) the modified control parameter $1/B'$ for all viscosities (V02, V05, V10, V20 and V100) and different cell geometries: •, $b = 1.43$ mm, $W = 4$ cm; ×, $b = 0.75$ mm, $W = 4$ cm; □, $b = 0.75$ mm, $W = 8$ cm; +, $b = 0.25$ mm, $W = 4$ cm.

parameter, again for $We_c^* = 15$. We observe that the entire data set collapses very well onto a single master curve. Once again this curve is identical to the classical result of McLean & Saffman (1981).

So far we have not discussed the influence of the aspect ratio on the relative finger width. Even if the influence is small, it might explain why we observe slight differences between the four different cell geometries (see figure 6b). In contrast, when considering one single channel geometry the data do collapse (see figure 5). If one also notes that these differences can be observed where inertia is negligible, the conclusion must be that the slight residual differences are due to film effects. These effects are also responsible for the slight decrease of the finger width below $\lambda = 0.5$ (see Tabeling *et al.* 1987) observed on figure 6(b).

The physical interpretation of our results is then the following. The modified control parameter $1/B'$ gives the crossover between the $1/B$ and Re^* regimes. For small We^*, $1/B$ is the control parameter, and the main forces are surface tension and viscous forces, leading to a narrowing of the fingers as viscous forces become more important for higher speeds. For higher velocities ($We^* > We_c^*$), the main forces acting are viscous forces and inertia. The competition between these forces results in a widening of the fingers with increasing velocity. The observation is therefore that inertia tends to widen the fingers; this seems logical intuitively, as the inertia will tend to slow down the finger at a given flow rate, leading to wider fingers. As the effect of the inertial forces is similar to that of the capillary forces, in the sense that both tend to widen the finger, and as the classical Saffman–Taylor finger selection appears to have remained intact, one may attempt to include the inertial forces in an effective surface tension. Indeed the modified control parameter $1/B'$ can be written as the classical control parameter $1/B$ by including an effective surface tension that is of the form

$$\gamma_{eff} = \gamma(1 + We^*/We_c^*), \tag{4.5}$$

leading to the same data collapse as shown in figures 5 and 6(b).

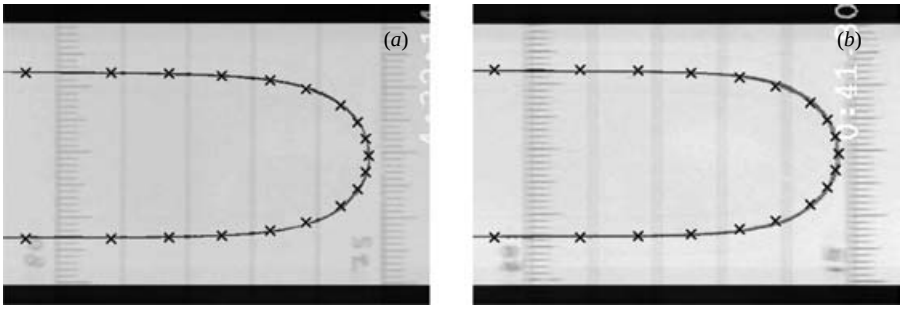

FIGURE 7. Snapshot of a finger of $\lambda = 0.63$: (*a*) without inertial effects ($We^* = 5 < We_c^*$, silicon oil V02, velocity $U = 5.2\,\mathrm{cm\,s^{-1}}$, $b = 0.75\,\mathrm{mm}$, $W = 4\,\mathrm{cm}$); (*b*) with inertial effects ($We^* = 30 > We_c^*$, silicon oil V02, velocity $U = 12.5\,\mathrm{cm\,s^{-1}}$, $b = 0.75\,\mathrm{mm}$, $W = 4\,\mathrm{cm}$). ×, Finger shape ($\lambda = 0.63$) predicted without inertial effects by the theory of Pitts (1980).

5. Some theoretical elements

The experimental observations also indicate that even though the finger width increases when increasing the velocity sufficiently the finger shape does not really change. Figures 7(*a*) and 7(*b*) show finger shapes for identical $1/B'$ (within 5 %) and thus identical width ($\lambda = 0.63$), but with (figure 7*b*) or without inertial effects (figure 7*a*). We have compared their shapes to the prediction of Pitts (1980) for classical Saffman–Taylor fingers not taking inertial effects into account. The experimental finger shapes are in good agreement with this prediction. This indicates that, for the same width, the finger shape is not modified by inertia. These observations hold for all experiments.

All these observations suggest the possibility of introducing the inertial effects in a perturbative manner into the framework of the classical Saffman–Taylor treatment of the viscous fingering instability. We thus choose to simply use a modified Darcy law.

5.1. *Perturbation of Darcy's law*

Modifications of Darcy's law have already been introduced in § 2.2. We will now consider the Euler–Darcy equation and thus a Darcy equation corrected by inertia, in the frame of the moving finger.

One starts from (2.5) for the two-dimensional velocity field $\boldsymbol{u}(x, y, t)$ in the laboratory frame. In the frame of the moving finger the problem is by definition stationary. Taking $\boldsymbol{u}(x, y, t) = \boldsymbol{u}'(x - Ut, y) + U\boldsymbol{e}_x$, we obtain for the velocity $\boldsymbol{u}'(x, y)$ in the frame of reference of the moving finger:

$$\rho\left(-\alpha U\frac{\partial \boldsymbol{u}'}{\partial x} + \beta U\frac{\partial \boldsymbol{u}'}{\partial x} + \beta \boldsymbol{u}'\cdot\nabla\boldsymbol{u}'\right) = -\nabla p - \frac{12\eta}{b^2}(\boldsymbol{u}' + U\boldsymbol{e}_x). \tag{5.1}$$

Using the same scaling as before and omitting the * (dimensionless symbols) and the prime (finger frame) for the variables, we find

$$Re^*\left((\beta - \alpha)\frac{\partial \boldsymbol{u}}{\partial x} + \beta\boldsymbol{u}\cdot\nabla\boldsymbol{u}\right) = -\nabla p - \boldsymbol{u} - \boldsymbol{e}_x. \tag{5.2}$$

We assume that the flow remains a potential flow, i.e. $\boldsymbol{u} = \nabla\phi$. This restriction to potential flow without vorticity is possible as long as the boundary conditions that

apply to the finger and the walls are not modified. If this is the case, one can write

$$\phi = -\left[p + Re^* \left[(\beta - \alpha)u_x + \tfrac{1}{2}\beta u^2\right] + x + \text{const}\right] \quad \text{and} \quad \Delta\phi = 0. \tag{5.3}$$

Assuming that along the finger and away from its tip there are no inertial effects (the fluid is at rest in the laboratory frame, and $\lim_{x\to-\infty} \boldsymbol{u} = -e_x$ in the finger frame) one should choose the constant equal to $Re^*(\beta/2 - \alpha)$.

Note that in the far field, away from the finger interface, $\boldsymbol{u}$ is uniform and we deduce from (5.3):

$$\boldsymbol{u} = \nabla\phi = -\nabla p - 1, \tag{5.4}$$

which leads to the classical Darcy law in the laboratory frame.

The mechanical equilibrium of the interface requires the balance of the normal stress from both sides, given by (2.3): $p = -\tilde{\gamma}/R$ $(R > 0)$, where $\tilde{\gamma} = (b/W)^2\gamma/(12\eta U) = 1/B^{-1}$ is the dimensionless surface tension and R is the dimensionless radius of curvature. Using this, one obtains the following boundary condition for ϕ at the interface:

$$\phi_\Gamma = -\left[-\tilde{\gamma}/R + Re^*\left[(\beta - \alpha)u_x + \tfrac{1}{2}\beta u^2 + \beta/2 - \alpha\right] + x\right]. \tag{5.5}$$

As the normal velocity at the interface u_n is zero in the frame of the moving finger, the only remaining velocity component is the tangential one u_t and we can use the notation of McLean & Saffman (1981): $\boldsymbol{u} = u_t \boldsymbol{e_t} = -q(\cos\theta \boldsymbol{e_x} + \sin\theta \boldsymbol{e_y})$ where q varies from 0 (at the tip of the finger) to 1 (at its side) when θ varies from $-\pi/2$ to 0. We can thus replace u^2 by q^2 and $-u_x$ by $q\cos\theta$.

As q is mainly given by $\cos\theta$, one can write

$$\phi_\Gamma = -x + \tilde{\gamma}[1/R + We^*(\alpha - \beta/2)\sin^2\theta]. \tag{5.6}$$

Note that the last term is the Bernoulli correction. In a different context, potential flows using Bernoulli's equation (for $Re \to \infty$) have been extensively studied in the past (see Garabedian 1957, 1985; Vanden-Broeck 1984, 2004). These studies mainly concern ascending bubbles (see Garabedian 1957, 1985; Vanden-Broeck 1984) or cavitating flows around obstacles (see Vanden-Broeck 2004). However, their results cannot be directly compared to our study.

In (5.6), according to Gondret & Rabaud (1997), Ruyer-Quil (2001) and Plouraboue & Hinch (2002), $(\alpha - \beta/2)$ is positive, so that this correction has the same sign as the curvature. It also vanishes at the sides of the finger. This shows that the effect of the inertial term is very similar to that of the capillary forces: the inertial forces should tend to increase the finger width, as was indeed observed experimentally.

Finally, rewriting (5.6), it follows that

$$\phi_\Gamma = -x + \hat{\gamma}(\theta)/R, \quad \text{with} \quad \hat{\gamma}(\theta) = \tilde{\gamma}[1 + We^*(\alpha - \beta/2)R(\theta)\sin^2\theta]. \tag{5.7}$$

This equation is reminiscent of (4.5) obtained above by considering the modified control parameter $1/B'$ with an effective surface tension.

5.2. *Numerical simulations and comparison to experimental data*

Of course the selection of the relative width of the finger can only be found by a sophisticated singular perturbation analysis. However, the relative finger width can be obtained numerically by a modification of the McLean & Saffman (1981) method. We choose this method for a comparison with the experimental results and introduce the correction of Ruyer-Quil (2001) in the numerics using (5.5). We corrected for the

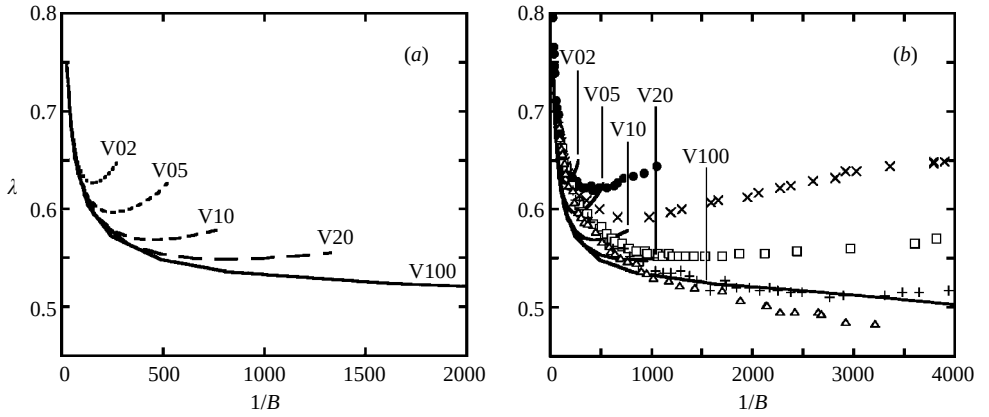

FIGURE 8. Finger width λ as a function of the classical control parameter $1/B$ for the geometry with $b = 0.75$ mm and $W = 4$ cm and different fluids: (*a*) numerical simulations and (*b*) comparison between simulations and experimental results, experimental data: •, V02; ×, V05; □, V10; + V20; △, V100; numerical simulations: lines.

thin film effect in the simplest way possible: we modified the value of the surface tension to what has been proposed by Tabeling & Libchaber (1986). For the film thickness we used (4.2) which does not take inertia into account.

If this is done, the numerical simulations confirm the simple argument pointed out above and show an increase of the relative finger width compared to the classical results (see figure 8*a*), in agreement with the experiments. The observations from the numerical results are:

(i) the inertial effects are stronger (i.e. appear for a smaller critical $1/B$) for less viscous fluids as well as for larger cell thickness or for smaller cell width;

(ii) the minima of the relative width as a function of We^* are around a unique value of We_c^*, however the numerical value of We_c^* differs between the experiments (≈ 15) and the simulations (≈ 2).

Comparison of the simulations and the experiments (see figure 8*b*) shows that they are in qualitative agreement but that the results are not identical.

When inertial effects are present we can characterize these effects by estimating a critical value of the control parameter $1/B_c$ and a critical relative width λ_c at the minimum. The numerics provide a rather good estimate for λ_c but fail to give a correct value for $1/B_c$ which is found to be smaller in the numerical simulations than in the experiments. Another significant difference is that the increase of the λ–$1/B$ curve is observed to be stronger in the simulations.

However, even for the case where inertia can be neglected (for the most viscous fluid), there is a small but significant discrepancy between the numerical simulations and the experimental data. We believe this is due to the fact that our way of correcting for the wetting film is too simple. As a consequence, it is clear that we cannot expect perfect agreement between experimental data and simulations when adding corrections due to inertia. To quantitatively account for the experimental results, one has to go back to the three-dimensional effects of the experiment which are expected to be important close to the finger tip over a length scale of order b. This is due to the existence of a three-dimensional structure of the flow which cannot be ignored in the vicinity of the finger: a film exists between the plate and the finger. Park & Homsy (1984) and Reinelt & Saffman (1985) have shown that it is nevertheless possible to

reduce the problem to two dimensions by modifying the boundary conditions on the finger (see also Ben Amar & Rice 2002). However, they have also shown that reduction to two dimensions is only possible if the parameter $We = \rho U^2 b/\gamma$ is small. For our problem, this is not the case and therefore a complete set of the corrected boundary conditions must be deduced from the full three-dimensional theory of Park & Homsy and Reinelt & Saffman incorporating inertial effects in order to resolve the problem, which is beyond the scope of this paper.

6. Summary and conclusion

We have investigated the effect of inertia on the Saffman–Taylor instability. Inertial effects are found to become important for fluids of low viscosity and for large plate spacing of the Hele-Shaw cell. For these situations one observes, upon increasing the velocity, first a classical regime with a decrease of the relative finger width and then a second and new regime in which the finger width increases. This second regime is due to the importance of inertia.

We introduced a modified Weber number We^* which allowed us to explain the crossover between the two regimes. The transition is thus given by a critical modified Weber number We^*_c. Below We^*_c, the classical regime of decreasing finger width is of course governed by the classical control parameter $1/B$, which is a modified capillary number. The finger width in this regime is thus given by the balance between capillary forces, which tend to widen the finger, and viscous forces, which tend to narrow the finger. With increasing velocity the viscous forces dominate over the capillary forces and one observes a narrowing of the finger. For the second regime, above We^*_c, one observes on the contrary an increase of the finger width with increasing velocity. In this case the finger width is governed by a modified Reynolds number Re^* and thus by the balance between viscous forces and inertia. It turns out that inertial forces tend to widen the finger. With increasing velocity inertia dominates the viscous forces and one consequently observes a widening of the fingers.

We have also shown that we can define a new control parameter $1/B'$, which takes the corrections due to inertia into account. This parameter tends towards $1/B$ for low We^* and is proportional to $1/Re^*$ for large We^*. When plotting our data as a function of this empirical parameter they collapse onto a single universal curve which corresponds to the results for the finger width obtained for the classical Saffman–Taylor instability.

By only taking into account a modification of Darcy's law, some simple arguments and numerical simulations confirm all of these observations. However, the agreement between numerics and experiments is only qualitative. We believe this is due to the fact that the problem is certainly three-dimensional and one must consider the full three-dimensional theory of Park & Homsy and Reinelt & Saffman incorporating inertial effects.

It may be interesting to investigate whether inertia modifies the tip splitting instability observed classically for high value of the control parameter $1/B$. To do so it would be appropriate to work in an open (circular) geometry. One could then also compare to a linear stability analysis for a planar interface when taking inertia into account.

We thank Eric Clément, Mike Shelley and Laurent Limat for useful discussions and José Lanuza for valuable help with the experimental set-up.

REFERENCES

Ben Amar, M. & Rice, J. R. 2001 Exact results with the J-integral applied to free-boundary flows. *J. Fluid Mech.* **461**, 321–341.

Bensimon, D., Kadanoff, L. P., Liang, S. D., Shraiman, B. I. & Tang, C. 1986 Viscous flows in 2 dimensions. *Rev. Mod. Phys.* **58**, 977–999.

Bonn, D., Kellay, H., Ben Amar, M. & Meunier, J. 1995 Viscous finger widening with surfactants and polymers. *Phys. Rev. Lett.* **75**, 2132–2135.

Combescot, R., Dombre, T., Hakim, V., Pomeau, Y. & Pumir, A. 1986 Shape selection of Saffman–Taylor fingers. *Phys. Rev. Lett.* **56**, 2036–2039.

Couder, Y. 1991 Growth patterns: from stable curved fronts to fractal structures. In *Chaos, Order and Patterns* (ed. R. Artuso, P. Cvitanovic & G. Casati). Plenum.

Garabedian, P. R. 1957 On steady-state bubbles generated by Taylor instability. *Proc. R. Soc. Lond.* A **241**, 423–431.

Garabedian, P. R. 1985 A remark about pointed bubbles. *Commun. Pure Appl. Maths* **38**, 609–612.

Gondret, P. & Rabaud, M. 1997 Shear instability of two-fluid parallel flow in a Hele-Shaw cell. *Phys. Fluids* **9**, 3267–3274.

Homsy, G. M. 1987 Viscous fingering in porous-media. *Annu. Rev. Fluid Mech.* **19**, 271–311.

Hong, D. C. & Langer, J. S. 1986 Analytic theory of the selection mechanism in the Saffman–Taylor problem. *Phys. Rev. Lett.* **56**, 2032–2035.

Kawaguchi, M., Hibino, Y. & Kato, T. 2001 Anisotropy effects of Hele-Shaw cells on viscous fingering instability in dilute polymer solutions. *Phys. Rev.* E **64**, 051806.

Lindner, A., Bonn, D. & Meunier, J. 2000 Viscous fingering in a shear-thinning fluid. *Phys. Fluids* **12**, 256–261.

Lindner, A., Bonn, D., Poire, E. C., Ben Amar, M. & Meunier, J. 2002 Viscous fingering in non-Newtonian fluids. *J. Fluid Mech.* **469**, 237–256.

McLean, J. W. & Saffman, P. G. 1981 The effect of surface-tension on the shape of fingers in a Hele Shaw cell. *J. Fluid Mech.* **102**, 455–469.

Park, C. W. & Homsy, G. M. 1984 Two-phase displacement in Shaw-Hele cells: theory. *J. Fluid Mech.* **139**, 291–308.

Pitts, E. 1980 Penetration of fluid into a Hele Shaw cell. *J. Fluid Mech.* **97**, 53–64.

Plouraboue, F. & Hinch, E. J. 2002 Kelvin-Helmholtz instability in a Hele-Shaw cell. *Phys. Fluids* **14**, 922–929.

Reinelt, D. A. & Saffman, P. G. 1985 The penetration of a finger into a viscous-fluid in a channel and tube. *SIAM J. Sci. Stat. Comput.* **6**, 542–561.

Ruyer-Quil, C. 2001 Inertial corrections to the darcy law in a Hele-Shaw cell. *C. R. Acad. Sci. Paris* IIb **329**, 337–342.

Saffman, P. G. & Taylor, G. 1958 The penetration of a fluid into a porous medium or Hele-Shaw cell containing a more viscous liquid. *Proc. R. Soc. Lond.* A **245**, 312–329.

Shraiman, B. I. 1986 Velocity selection and the Saffman–Taylor problem. *Phys. Rev. Lett.* **56**, 2028–2031.

Smith, D. E., Wu, X. Z., Libchaber, A., Moses, E. & Witten, T. 1992 Viscous finger narrowing at the coil-stretch transition in a dilute polymer-solution. *Phys. Rev.* A **45**, R2165–R2168.

Tabeling, P. & Libchaber, A. 1986 Film draining and the Saffman–Taylor problem. *Phys. Rev.* A **33**, 794–796.

Tabeling, P., Zocchi, G. & Libchaber, A. 1987 An experimental-study of the Saffman–Taylor instability. *J. Fluid Mech.* **177**, 67–82.

Vanden-Broeck, J. M. 1984 Bubbles rising in a tube and jets falling from a nozzle. *Phys. Fluids* **27**, 1090–1093.

Vanden-Broeck, J. M. 2004 Nonlinear capillary free-surface flows. *J. Engng Maths* **50**, 415–426.

Vlad, D. H. & Maher, J. V. 2000 Tip-splitting instabilities in the channel Saffman–Taylor flow of constant viscosity elastic fluids. *Phys. Rev.* E **61**, 5439–5444.